INTERACTION BETWEEN WIND-DRIVEN AND BUOYANCY-DRIVEN NATURAL VENTILATION

Bo Wang, Foster and Partners, London, UK

ABSTRACT

Ventilation stacks are becoming increasingly common in the design of naturally ventilated buildings. Maintaining a certain airflow direction is crucial for a successful natural ventilation design.

This article presents the experimental and theoretical investigation of unsteady wind effects on natural ventilation of a single envelope with multiple openings for wind and buoyancy combined cases. Wind tunnel tests have been carried out to investigate the hysteresis effects, the effects of turbulent wind pressure fluctuations on stack flow rates, and the initial condition effects on the final flow pattern through multiple stacks.

It has been confirmed experimentally that when the wind and buoyancy forces are in opposition and nominally equal, the turbulent wind fluctuation could cause effective ventilation rates. When there are only stacks open with a fixed buoyancy force, the flow directions through the stacks depend on the initial conditions; which indicates the uncertainty in CFD simulation due the input of initial conditions.

INTRODUCTION

When buoyancy exists, in theory the flow condition within a single zone space can be classified into two categories, which are 1) buoyancy alone; 2) buoyancy and wind combined. When buoyancy is acting alone, or wind is assisting buoyancy source; it is relatively simple. This paper will focus on wind apposing buoyancy cases.

There are two types of buoyancy source: localised heat source and area heat source (e.g. a heated floor). Linden et al (Hunt and Linden, 1999; Hunt and Linden, 2001; Hunt and Linden, 2004) studied the localised heat source buoyancy ventilation. A Series of buoyancy ventilation cases were studied by Woods et al (Gladstone and Woods, 2001; Lishman and Woods, 2006); but their laboratory work was using a heated floor which was an area heat source. Multiple local heat sources and different heights of heat source were also studied (Chenvidyakarn and Woods, 2010; Fitzgerald and Woods, 2004; Livermore and Woods, 2007).

For cases of area heat source, the room temperature will achieve uniformity as a steady state. Thermal stratification occurs with localised heat source when air enters in a lower opening and exits from an upper opening. This is defined as displacement ventilation or buoyancy domain ventilation. When the opposing wind is strong enough that pressure difference due to wind across openings are greater than that due to buoyancy, mixing ventilation will occur, which is also called wind domain ventilation (Hunt and Linden, 2004) (see Figure 1).

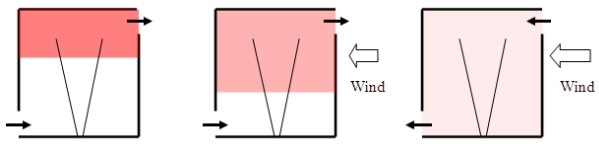

Figure 1 Localised heat source ventilation: (1) displacement ventilation driven by a localised heat source alone; (2) displacement ventilation driven by buoyancy and opposing wind; (3) mixed ventilation driven by buoyancy and strong opposing wind.

A theoretical model was developed to estimate the steady-state interface heights, stratification profiles and ventilation flow rates for this kind of heat source. It was found that the interface height is independent of the strength of the buoyancy flux from the source, but decided by the effective opening area. An increase in the heat flux will increase the upper layer temperature but not change the height of the layer. With a fixed heat flux, the weak apposing wind will increase the thickness of the upper layer, yet decrease its temperature. Information of details of heat and mass transfer between stratification layers can be found in the literature (Turner, 1973). CFD modelling was studied by Ji et al. (2007), in which a localised heat source was used; thermal stratifications were predicted. The effects of size and location of ventilation openings, distribution of heating sources and wind strength on flow rates and temperature distribution were studied.

Hunt and Linden (2004) also investigated in the transitions between two ventilation flow patterns: buoyancy domain/displacement ventilation and wind domain /mixing ventilation. A localised heat source was used in this study theoretically and experimentally. Both buoyancy and wind forces were adjusted to generate different steady states. A dimensionless parameter F was defined, which is the relative magnitudes of the wind-driven velocity component and the buoyancy-driven velocity component within the enclosure. It was found that transitions between the two flow patterns exhibit hysteresis. The tests carried out in this paper also exhibit hysteresis, which will be discussed in the experiment results and analysis. In terms of transition requirement, it was discovered that mixing to displacement ventilation occurs at a fixed value of F, whereas the opposite transition from displacement to mixing ventilation is not solely depend on the value of F but also on some other details such as time history of the flow and the geometry of the openings.

Similar results were discovered by Lishman and Woods (2009). The differences are: area heat source was used; only wind driving force was changed to generate different steady states. Again, it was stated that the transition from the wind dominated to buoyancy dominated mode occurs as the wind force decreases below a critical value, which is corresponding the fixed value of *F* in Linden's study. Similarly the opposite transition from buoyancy dominated to wind dominated mode occurs if there is a sufficiently large and rapid increase in the wind force.

Yuan and Glicksman (2007) theoretically investigated the transition between the two steady modes, in terms of perturbation of both heat source and wind source. It was found that a minimum perturbation magnitude and minimum perturbation time should be satisfied to make the transition happen. It was also suggested that special attention should be paid to wind perturbation which is more likely to occur in practice.

The transition studies in literature were all based on a typical building with two sharp openings. In this paper, transition on a model with long opening will be studied, in which the process of transition can be 'slowed down'.

PARTS OF THE PAPER

Experiment description

The same model used in Wang et al. (2011) was used for buoyancy and wind combined tests. A heater was fixed in the centre of the bottom (see Figure 2), the dimension of the heater is 12 cm wide, 12 cm long and 2.5 cm high. With a manually controlled power supply of 110~250 V, the heater generates a heating range of 60~200 W. There is a temperature probe (Dantec 55P33) fitted below the hot-wire in one of the four stacks (stack 3), to measure the ambient temperature of the hot-wire for instantaneous temperature corrections. To measure the box temperature, there are two thermocouples fixed within the space. One is 0.8 of the box height, the other is 0.25 of the box height, and both of them are half way distance to the centre in opposite corners. There is third thermocouple located under the turntable of the wind tunnel to measure the ambient environment temperature. The data acquisition of the temperature probe in the stack is the same system with the hot-wires, thereby the velocity and correction temperature measurements are synchronized. The data acquisitions of the three thermocouples are using a data logging system. The temperature measurements of the thermocouples were recorded simultaneously with the hot-wires, the error of the synchronization is up to one second. The temperatures measured by the three thermocouples and temperature probe are called T_1, T_2, T_{room} and T_{wire}. It should be noted that no correction is required for detecting flow reversal, correction is only required for calculating the magnitude of the flow rate.

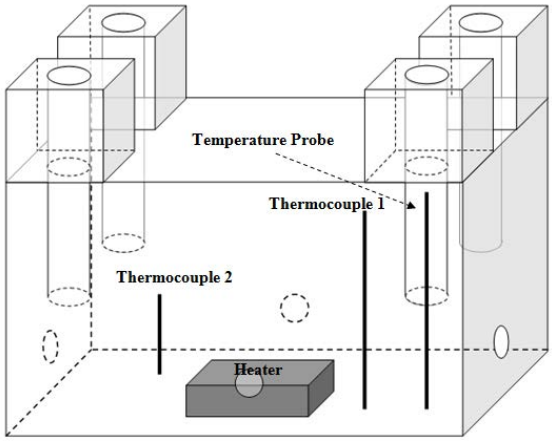

Figure 2 Model with heater and temperature measurements

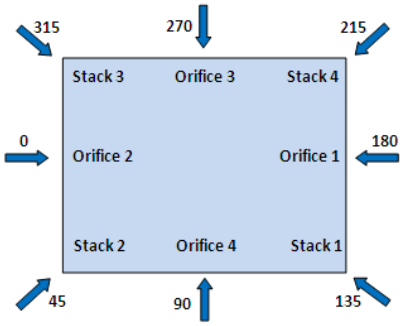

Figure 3 Plan view of stack and orifice positions, with wind direction

Similarity analysis

There are certain dimensionless parameters regarding similarity requirements, namely Reynolds number and Archimedes number (Carey and Etheridge, 1999). The two relevant Reynolds numbers, namely building Reynolds number and opening Reynolds number, are defined by equation (1) and equation (2)

$$Re_b = \frac{\rho_{E0} U_{ref} H}{\mu} \quad (1)$$

$$Re_o = \frac{\rho_{E0} u d}{\mu} \quad (2)$$

The Archimedes number is defined by

$$Ar = \frac{\Delta\rho g h}{\rho_{E0} {U_{ref}}^2} = \frac{\Delta T g h}{T_{E0} {U_{ref}}^2} \quad (3)$$

where ρ_{E0} is the external air density at 0 height. $\Delta\rho$ is the density difference at a specified opening height, and ΔT is the temperature difference at the specified opening height.

A dependence of envelope flows on Re_b can be considered in two parts i.e. dependence of external pressure coefficient, C_p on wind tunnel speed (Re_b) and dependence of the discharge coefficient on flow rate (Re_o). For a long opening, C_z is dependent on Re_o especially at low flow rate. From the results in Wang et al. (2011), we know that C_p is independent of the

wind speed when U_{ref} is greater than 3 m/s at model scale. Assume that one knows the dependency equation for C_z and Re_o for full scale. Also, C_p values at low wind speed for full scale buildings could be provided, or the dependency on wind speed is small enough to be ignored. There left only one important requirement for buoyancy and wind combined ventilation especially during the transition processes. To give the required ratio between buoyancy and wind forces, a prototype Archimedes number has to be achieved. In other words, to apply model scale results to full-scale, it is necessary to achieve full-scale values of Ar.

The advantage of using the salt-bath technique is that there is no problem achieving high Reynolds numbers and also satisfying the prototype Archimedes number. But the problem is with boundary conditions. The main advantage of the direct wind tunnel technique is that the atmospheric boundary layer can be more accurately modelled in an environmental wind tunnel than in a water channel (Carey and Etheridge, 1999). By using air, one has to use a high temperature difference and/or a low wind speed to achieve full-scale Ar. An example of applying model scale results to full-scale is given as follows. Assume there is a geometric scaled building 50 times of the height of the box; the temperature difference between the inside and outside of the building is 5 ℃; full scale wind speed is 3m/s. At model scale with a temperature of 30 ℃, $\frac{5K \times g \times 50}{300K \times (3m/s)^2} = \frac{30K \times g \times 1}{300K \times U^2}$, the wind speed U_{ref} has to be as low as about 1 m/s to satisfy the prototype Archimedes number.

Experiment scope

The aims of the experiments are: 1) to investigate the transitional processes between wind dominated and buoyancy dominated states, and to study the hysteresis effects; 2) to investigate the effects of turbulent wind pressure fluctuations on stack flow rates; 3) to investigate the initial condition effects on the final flow pattern through multiple stacks.

As stated in the similarity analysis, the temperature difference between the box and ambient room temperature should be as large as possible. Although the working environment of the hot-wire can be as high as 150 ℃, the precise range of the temperature probe is below 60 ℃, and temperature is also limited by the power of the heater. The tests carried out in this chapter are all below 65 ℃.

In the first test, the two measured temperatures from the thermocouples (the temperature within the model was stratified) were set constant, and the wind speed was adjusted to produce the transitions from buoyancy dominated ventilation to wind dominated ventilation on the opening configuration of two stacks and four orifices. In the second test, the wind speed was set constant, and the heater was adjusted up and down to produce the transitions from wind dominated ventilation to buoyancy dominated ventilation on the opening configuration of one stack and one orifice. What is more, stacks alone tests were carried out to investigate the initial condition effects. Details of experimental scope are shown in Table 1.

Table 1 Experimental scope of wind and buoyancy combined tests

1. **FIXED TEMPERATURE IN THE BOX**			
T_1, T_2 (℃)	U_{ref} range	Openings	Identifier
60, 40	1.2 ~ 1.7	Stack 1 and 3, Orifice 1 2 3 4	S13_O1234_T57
57, 42	1.2 ~ 2.1	Stack 1 and 3, Orifice 1 2 3 4	S13_O1234_T60
2. **ONE STACK AND ONE ORIFICE, FIXED**			
U_{ref} (m/s)	T_2 range (℃)	Openings	Identifier
0.6	16 ~ 60	Stack 3, Orifice 1	S3_O1_U0.6
3. **INITIAL CONDITION EFFECT TESTS**			
T_2 (℃)	U_{ref} (m/s)	Openings	Identifier
60	1.7	Stack 1 and 3	S13_T60
60	4	Stack 1 2 3 4	S1234_T60
60	4	Stack 1 2 3 4, Orifice 1	S1234_T60

Experiment results and analysis

Transition from buoyancy dominated ventilation to buoyancy dominated ventilation

The changing of flow directions are shown in Figure 4. Starting with only a fixed buoyancy force, the flow direction in stack 3 is upward, i.e. the reversal percentage r of stack 3 is 0 %. By gradually increasing the wind speed of the wind tunnel, the flow through stack 3 starts to fluctuate; r starts to increase from 0 % till 100 % (flow direction sign from - to +), when the wind force is great enough to make the flow direction of stack 3 totally change to downward. After the fan was switched off, the flow direction of stack 3 gradually turned back to upward again to its original status (flow direction sign from + to -).

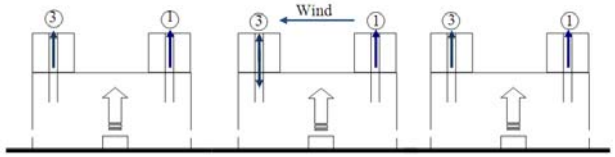

Figure 4 Transitions from displacement ventilation to mixing ventilation, and then back to displacement ventilation

The quantitative results are shown in Figure 5 and Figure 6. The main y axis shows the temperatures

and reversal percentage, the secondary *y* axis is the wind speed. Since the wind speed was increased manually, the results are not presented in the form of time slots. The *x* axis is just a number of records; the time interval is about three minutes. *Figure*5 shows the results of fixed upper layer model box temperature measured by thermocouple 1: $T_1 = 57$℃; Figure 6 shows the results of $T_1 = 60$℃. One can see that with a higher T_1 by 3℃, the wind speed has to reach 2.1 m/s to cause 100% flow reversal in stack 3, whereas it is 1.7 m/s in *Figure*5.

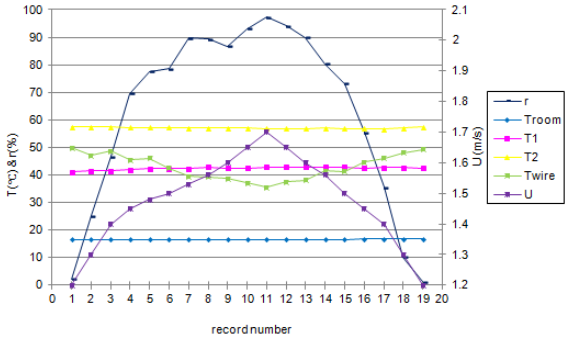

Figure 5 Variation of temperature and reversal percentage of stack 3 for T1 =57 ℃ (S13_O1234_T57)

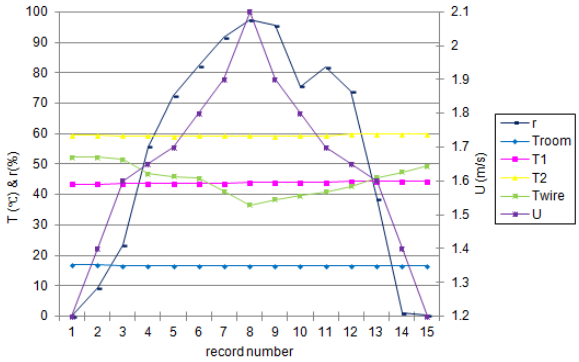

Figure 6 Variation of temperature and reversal percentage of stack 3 for T1 =60 ℃ (S13_O1234_T60)

Figure 7 shows the results of reversal percentage changes with increasing and decreasing wind speed for the above two cases of $T_1 = 57$ ℃ and $T_1 = 60$ ℃ ('- to+' means the change of flow sign in stack 3). Again, no obvious hysteresis effects could be observed between the two processes. Lishman and Woods (2009) stated that , for the typical one zone building with two openings, transition from the wind dominated state to buoyancy dominated state occurs as the wind force decreases below a critical value. However they stated that the reverse transition (from buoyancy dominated to wind dominated state) occurs only if there is a sufficiently large and rapid increase in the wind force. In this paper, the two transition processes happen with a gradually changing wind speed. The possible explanation could be that the long stack slows down the transitional process, thereby mitigating the need of the sudden jumping of the wind force to transit from buoyancy dominated state to wind dominated state.

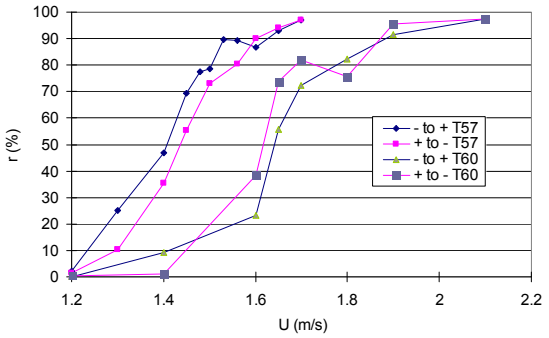

Figure 7 Reversal percentage against wind speed

In addition, from Figure 5 and Figure 6, one can see that when buoyancy force was fixed, in the stacks through which flow direction change, the fluctuation through the stack is more severe when the wind force was increasing; the reversal percentage changes more smoothly when the wind force was receding. Yet this phenomenon was not observed when the wind force was fixed and buoyancy force was changing, in which case the reversal percentage changed relatively smoothly during both processes of increasing and decreasing buoyancy force.

Transition from wind dominated ventilation to buoyancy dominated ventilation

The aim of these tests was to provide confirmation of the effect of turbulence as described in Etheridge (2009). As shown in Figure 8, a wooden block was put on top of the model to generate an initial downward flow in stack 3, a wind dominated ventilation state, with $U_{ref} = 0.6\,m/s$. After the heater was turned on, the flow direction in stack 3 started to change from downward to totally upward. Temperatures and reversal percentage change with time can be found in Figure 9.

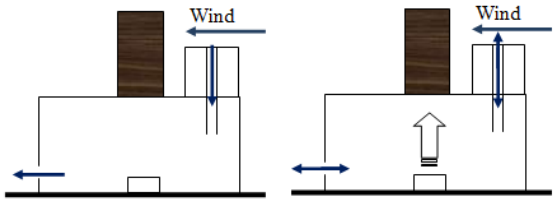

Figure 8 Transition from wind dominated ventilation to buoyancy dominated ventilation

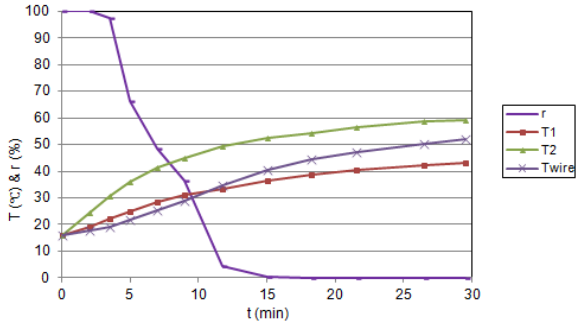

Figure 9 Temperatures and flow direction change with time

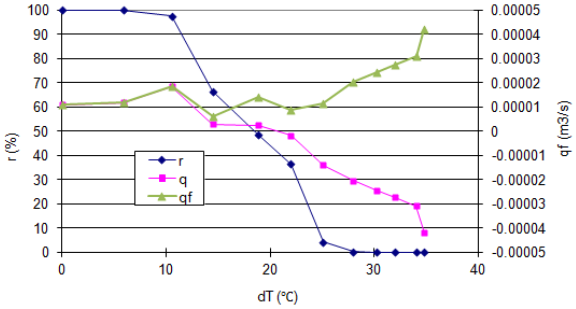

Figure 10 Reversal percentage, flow rate of stack 3 (q) and ventilation flow rate (fresh air) of the box (qf) against temperature difference

To give the correct velocity through the stack, temperature corrections are made to hot-wire calibration equations. The corrected voltage E_{corr} used to calculate velocities are obtained using equation (4) (Jorgensen, 2002, p. 29)

$$E_{corr} = \left(\frac{T_w - T_0}{T_w - T_a}\right)^{0.5} \times E_a \qquad (4)$$

where E_a is the acquired voltage. T_w is the sensor hot temperature, which is 250 ℃ in for the tests in this paper. T_0 is the ambient reference temperature related to the last overheat set-up before calibration, which is around 16 ℃ in the tests. T_a is the ambient temperature during acquisition, which is measured by the temperature probe in stack 3.

Figure 10 shows the reversal percentage, flow rate of stack 3 and total ventilation flow rate against temperature difference between the box and the room. Assuming that the flows through the two openings (stack 3 and orifice 1) are always equal and opposite, and also the air coming in each of the opening will mix entirely with the air inside the box, the fresh air ventilation rate is given the absolute value of either one of the two openings. Thereby the fresh air flow rate q_f used here is the mean absolute flow rate q of stack 3. However, in practice, the air coming in the opening will not entirely mix with the air inside the box, especially when it is fluctuating (when r is around 50 %) through the long opening (stack 3). Therefore the total ventilation rate with r around 50 % should be lower than that shown in the figure, but still not reaching zero. This is caused by the nature of the unsteadiness of the wind force. If one assumes that there is no fluctuation of the wind, the total ventilation rate would be zero when r = 50 %, which could not happen in practice.

Figure 11 illustrates the dimensionless total flow rate against relative dimensionless wind force and buoyancy force. The dashed line indicates what it should be were it for steady wind case. The dimensionless total flow rate is defined by

$$\frac{q_f}{AU_b} \qquad (5)$$

where q_f is the total flow rate, A is the area of the opening. U_b is the equivalent wind speed of the buoyancy force, which is defined by

$$U_b \equiv \sqrt{\frac{\Delta\rho g h}{\rho_{E0}}} \qquad (6)$$

The relative dimensionless wind force and buoyancy force is defined by

$$\frac{\Delta C_p}{Ar} \qquad (7)$$

where ΔC_p is the difference between the wind pressure coefficients of the two openings, since there are only two openings here. When there are multiple openings, Figure 11 should be used to analyse the quantities of each opening, thus in that situation ΔC_p should be the difference between the opening pressure coefficient and internal pressure coefficient. Ar is the Archimedes number which is defined by equation (3).

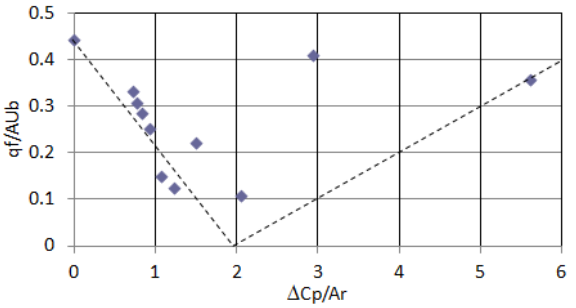

Figure 11 Dimensionless flow rate against relative wind force and buoyancy force

The dashed lines in Figure 11 correspond to the transition from wind dominated ventilation to buoyancy dominated ventilation. Etheridge (2009) stated that wind fluctuation should be severe enough

to eliminate the occurrence of multiple solutions when the term $\frac{\Delta C_p}{\sigma_{\Delta C_p}} < 1.5$, where $\sigma_{\Delta C_p}$ is the standard deviation of ΔC_p. In this study, $U_{ref} = 0.6\, m/s$, when $\frac{\Delta C_p}{\sigma_{\Delta C_p}} = 1.79$, which is not satisfying the requirement. However one should still see an effect, i.e. $\frac{q_f}{AU_b} > 0$ for $\frac{\Delta C_p}{\sigma_{\Delta C_p}} = 2$ and this is apparent in Figure 11. Nevertheless, higher wind speeds are suggested to be tested to satisfy the requirement, in which case a greater buoyancy force is needed to produce the transition to buoyancy dominated force, which is out of the range of the tests in this paper.

Figure 12 presents the results in the form of dimensionless ventilation rate $\frac{q_f}{A(U_{ref}+U_b)}$ against $1/Ar$, which is a way of providing non-dimensional data for design purposes (Carey and Etheridge, 1999). It should be noted that, the pressure data used for each point in the figures are taken from the wind alone case, when no buoyancy force component was present in the pressure measurements.

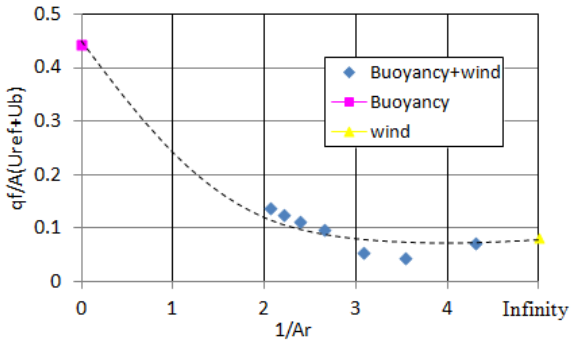

Figure 12 Dimensionless ventilation rate against 1/Ar

Initial condition effects

The aim here was to investigate the effect of initial conditions on the subsequent steady conditions.

For buildings with multiple stacks, there are uncertainties in the flow pattern arising from the effects of initial conditions. The flow directions through stacks in the final steady state with the same buoyancy force are likely to depend on the initial conditions such as the gust wind. Figure 13 shows the flow direction changes of two-stack alone case (stack 1 and stack 3). It started off with upward flow in stack 1 and downward flow in stack 3 when there was a constant temperature difference between the box and the room of 36 ℃. A wind speed of $U_{ref} = 2.5\, m/s$ caused the flow directions of the two stacks to completely change to the opposites. Ten minutes after the wind was switched off, when the driving force turned back to the original buoyancy alone state, the flow directions followed the status when the wind was on. This is presumably due to the cooling effect of the downward flow in stack 1. In the initial state, upward flow was established in stack 1, due to some asymmetry in the heating. If the asymmetry had been such that the flow in stack 1 was downward, there would have been no effect of wind. i.e. the thermal mass of stack 1 is cooled and therefore the flow in stack 1 remains downward.

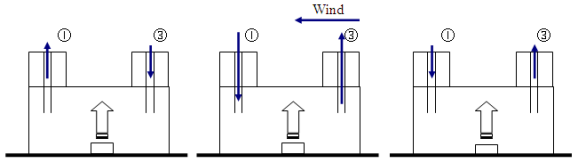

Figure 13 Initial condition effects of two-stack (stack 1 and stack 3) case

Results of the four-stack case are shown in Figure 14. The final flow directions in all four stacks follow the directions when the wind was on, $U_{ref} = 4\, m/s$. It should be noted that if the initial condition effect is due to cooling of thermal mass of the stack, it can not be simulated with the salt bath technique.

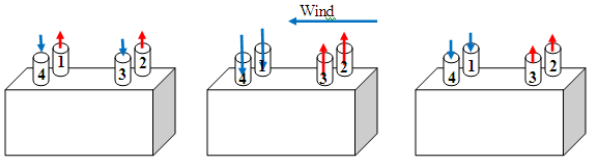

Figure 14 Initial condition effects of four-stack case

A question is raised: will the effects be the same when there are lower orifices open? Similar tests were carried out for the opening configuration of four stacks and one orifice (orifice 1). Results are shown in Figure 15. The final flow directions through the stacks do not follow the status when the wind was on ($U_{ref} = 4\, m/s$). The flow direction in stack 1 and 4 changes when there is wind, but returns to the original direction soon after U_{ref} turns back to 0 m/s. This is simply because air could come in the box through the lower orifice due to the pressure difference between the orifice outlet and stack outlets driven by buoyancy force alone. Bearing in mind the behaviour observed in Figure 14 and Figure 15, there is a value of the lower opening area for which the flow pattern will not return to its original state. The author carried out the same test shown in Figure 15, but sealed part of the opening area of orifice 1. The same flow pattern was obtained as that in Figure 14 untill the area was reduced to about 2.5 % compared to the stack areas. The porosity of lower orifice area has to be very small (less than 0.01%) for which the flow pattern would not return to its original state. Additionally, there could be different steady states of different flow directions within the stacks for the buoyancy alone case, when the lengths of the stacks are different. Results were obtained experimentally and theoretically in literature (Chenvidyakarn and Woods, 2005).

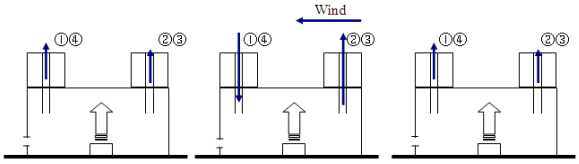

Figure 15 Initial condition effects of four stack and one orifice (Orifice 1)

SUMMARY AND CONCLUSIONS

Tests have been carried out to investigate the hysteresis effects, the effects of turbulent wind pressure fluctuations on stack flow rates, and the initial condition effects on the final flow pattern through multiple stacks. Main conclusions are as follows.

1) During the transitional process between buoyancy dominated and wind dominated states, the reversal percentage change relatively smoothly when wind force was fixed than when buoyancy force was fixed.

2) When transitions between different ventilation statuses happen in a model with long openings, there is no obvious hysteresis effect like what was stated in the literature, probably because the long opening could mitigate the transitioning process. More tests might be needed to prove this hypothetic conclusion.

3) In the one stack and one orifice tests when transition from wind dominated to buoyancy dominated ventilation happens, the influence of wind fluctuation eliminates the zero ventilation rate point, which in theory should exist regardless of the fluctuation of the driving forces. This supports the observation in Carey and Etheridge (1999)

4) When there are only stacks open with a fixed buoyancy force, the flow directions through the stacks could change due to an outside perturbation which could cause a new initial condition, like a gust wind (lasts long enough to change flow directions). However this will not happen when there are lower level openings of sufficient area.

NOMENCLATURE

A = Area of opening
Ar = Archimedes number
C_p = Pressure coefficient
ΔC_p = Difference of pressure coefficient
C_z = Discharge coefficient
g = Gravitational force per unit mass
H = Reference building dimension
P = Pressure
ΔP = Pressure difference
q = Volume flow rate through opening
Re_o = Opening Reynolds number
Re_b = Building Reynolds number
r = Time reversal percentage
t = Time
T = Temperature
u = Mean velocity through the opening
U (U_{ref}) = Reference velocity
z = Height of opening
ρ = Density
$\Delta\rho$ = Density difference
ΔT = Temperature difference y
μ = Viscosity
υ = Kinematic viscosity ($\upsilon = \mu/\rho$)
$\sigma_{\Delta Cp}$ = Standard deviation of ΔC_p
U_b = Buoyancy velocity

REFERENCES

Carey, P.S. & Etheridge, D.W. (1999). Direct wind tunnel modelling of natural ventilation for design purposes. Building Services Engineering Research and Technology.

Chenvidyakarn, T. & Woods, A. (2005). Multiple steady states in stack ventilation. Building and Environment, 40, 399-410.

Chenvidyakarn, T. & Woods, A. W. (2010). On the natural ventilation of two independently heated spaces connected by a low-level opening. Building and Environment, 45, 586-595.

Etheridge, D. W. (2009). Wind turbulence and multiple solutions for opposing wind and buoyancy. International Journal of Ventilation, 7, 309-319.

Fitzgerald, S. D. & Woods, A. W. (2004). Natural ventilation of a room with vents at multiple levels. Building and Environment, 39, 505-521.

Gladstone, C. & Woods, A. (2001). On buoyancy-driven natural ventilation of a room with a heated floor. Journal of Fluid Mechanics, 441, 293-314.

Hunt, G. R. & Linden, P. (1999). The fluid mechanics of natural ventilation--displacement ventilation by buoyancy-driven flows assisted by wind. Building and Environment, 34, 707-720.

Hunt, G. R. & Linden, P. (2001). Steady-state flows in an enclosure ventilated by buoyancy forces assisted by wind. Journal of Fluid Mechanics, 426, 355-386.

Hunt, G. R. & Linden, P. (2004). Displacement and mixing ventilation driven by opposing wind and buoyancy. Journal of Fluid Mechanics, 426, 355-386.

Ji, Y., Cook, M. J., & Hunt, G. R. (2007). CFD modelling of natural displacement ventilation in an enclosure connected to an atrium. Building and Environment, 42, 1158-1172.

Lishman, B. & Woods, A. (2006). The control of naturally ventilated buildings subject to wind and buoyancy. Journal of Fluid Mechanics, 557, 451-471.

Lishman, B. & Woods, A. W. (2009). On transitions in natural ventilation flow driven by changes in

the wind. Building and Environment, 44, 666-673.

Livermore, S. R. & Woods, A. W. (2006). Natural ventilation of multiple storey buildings: The use of stacks for secondary ventilation. Building and Environment, 41, 1339-1351.

Livermore, S. R. & Woods, W. (2007). Natural ventilation of a building with heating at multiple levels. Building and Environment, 42, 1417-1430.

Turner, J.S. (1973). Buoyancy effects in fluids. Cambridge University Press.

Wang, B., Etheridge, D.W., Ohba, M. (2011). Wind tunnel investigation of natural ventilation through multiple stacks. Part 1: Mean values. Building and Environment, 46, 1380-1392.

Yuan, J. & Glicksman, L. R. (2007). Transitions between the multiple steady states in a natural ventilation system with combined buoyancy and wind driven flows. Building and Environment, 42, 3500-3516.